INVESTIGATING LIGHTNING FLASH RATES IN TORNADIC ENVIRONMENTS

Ethan J. Kerr[1], Vanna C. Chmielewski[2], and Michael Stock[2,3]

[1]National Weather Center Research Experiences for Undergraduates Program
Norman, Oklahoma
[2]NOAA/OAR/National Severe Storms Laboratory
Norman, Oklahoma
[3]Cooperative Institute of Severe and High-Impact Weather Research and Operations, University of Oklahoma
Norman, Oklahoma

ABSTRACT

Lightning jumps, or a rapid increase in total flash rate, often precede severe weather and mesocyclogenesis. While there is plentiful research comparing lightning flash rates and general severe weather, there is less research on temporal relationships between flash rates and tornadogenesis in mixed storm modes. This study analyzes the total lightning flash rates of several dozen rotating cells from 12 tornadic environments from the PERiLS NSSL Lightning Mapping Array (LMA) deployments and the Oklahoma LMA. Cells were defined and tracked by their flash extent density. Comparative analyses were made between tornadic and non-tornadic cells, isolated supercells and cells embedded in quasi-linear convective systems (QLCSs), weak (EFU, EF0-1) and strong (EF2+) tornadoes, and time periods before and surrounding tornadogenesis. In a sample of 25 non-EF0, non-cyclic tornadoes, 80% were preceded by a 2-sigma lightning jump; however, more lightning jumps occurred in non-tornadic cells. When comparing flash rates before 31 tornadoes to peaks in low-level rotation in 19 non-tornadic storms, the tornadic storms experienced more total lightning. In a larger sample of 49 tornadoes, lightning flash rates were found to have steadily increased before tornadogenesis, peaking at around 17 minutes prior to tornado formation. After that, flash rates remained fairly steady across the sample. The difference in the change in flash rates before and after the 17 minute mark was statistically significant, providing confidence that an increase in flash rates precedes tornadogenesis. These results offer motivation for more research on lightning characteristics surrounding the evolution of tornadoes with larger sample sizes in the future.

1. INTRODUCTION

Previous research has found a positive relationship between rapid increases in lightning flashes and the onset of severe weather (Williams et al. 1999; Schultz et al. 2009). A rapid increase in total lightning with a thunderstorm is called a lightning jump. They don't always precede severe weather (wind, hail, tornadoes), but when they do they often happen 5-20 minutes before the occurrence of severe weather (Williams et al. 1999; Schultz et al. 2009). Lightning jump algorithms have been found to outperform NWS warning statistics when being used as a predictor for severe weather (Schultz et al. 2009). In supercells, lightning jumps are associated with an increase in mesocyclone rotation 85% of the time (Stough et al. 2017). However, limited research has analyzed the relationship between the occurrence of lightning jumps and tornadoes in rotating thunderstorms, especially of varying storm modes.

Perez et al. (1997) studied 42 supercells that produced violent (F4 and F5) tornadoes and found that 31 had a peak CG (cloud-to-ground) flash rate prior to tornadogenesis. Schultz et al. (2011) found that total lightning trends (the sum on intra-cloud and CG flashes) are a better predictor of severe weather than CG trends. Stough et al. (2017) consistently found lightning jumps before tornadogenesis or during the intensification of seven intense (EF3+) tornadoes. Williams and Carey (2015) analyzed four QLCS events. Two were tornadic and two were non-tornadic. They found that the tornadic cases had more total lightning and rotation. Additionally, lightning jumps preceded severe wind and tornadoes (Williams and Carey 2015). Despite a lack of research with large sample sizes into this relationship

[1] *Corresponding author address:* Ethan Kerr, Millersville University of Pennsylvania, OU CAPS, 120 David L. Boren Blvd, Suite 2500, Norman, OK 73072, Email: ethan.j.kerr@gmail.com.

specifically, meteorologists still use lightning jumps as a tool in tornado nowcasting.

Lightning is in the mixed-phase region of a cloud, which is the region between the 0°C and -40°C isotherms (Schultz et al. 2015). Here, electric charge is separated by colliding and rebounding graupel and ice crystals in the presence of supercooled water (Takahashi 1978). The differential sedimentation, stratification and turbulent rearrangement of charged particles creates regions of net charge. Intense updraft cores often associated with supercells are characterized by high flash rates of smaller flash areas due to the turbulent rearrangement of several complex charge regions in close proximity and large region supportive of particle electrification (Calhoun et al. 2013; Bruning and MacGorman 2013; Schultz et al. 2015). Schultz et al. (2015) found that lightning jumps are accompanied by increases in updraft volume and graupel mass in the mixed-phase region. Increases in peak updraft speeds were found with a majority of jumps, while updraft volume was correlated with total flash rate (Schultz et al. 2015).

Lightning production is generally a midlevel cloud process, and as such is influenced by the midlevel updraft characteristics. Similarly, a mesocyclone, which is a rotating updraft, is dependent on the midlevel updraft. Environmental horizontal vorticity arising from vertical wind shear is tilted vertically and stretched by a thunderstorm updraft, forming a mesocyclone (Markowski and Richardson 2009). Due to their shared dependence on the midlevel updraft, Stough et al. (2017) were able to correlate lightning jumps and mesocyclone strength. However, while all mesocyclonic tornadoes form under a mesocyclone, not all mesocyclones are associated with tornadoes. Tornadogenesis is significantly influenced by low-level and near-surface processes such as baroclinic vorticity generation and low-level wind shear (Markowski and Richardson 2014).

Due to the disconnect between the midlevel processes dominating lightning jumps and flash rates, and the additional low-level processes important to tornadogenesis, I hypothesize that lightning jump occurrence will not be an effective discriminator between tornadic and non-tornadic cells. However, within tornadic cells, I believe there could be a relationship between the occurrence of lightning jumps and tornadogenesis, because while a tornado requires more conditions to form than a mesocyclone, it is still reliant on the mesocyclone. I also hypothesize that total flash rate could differentiate tornadic and non-tornadic cells in a given environment with some accuracy due to its correlation with updraft speed or volume (Schultz et al. 2015).

A large sample of tornadic storms has yet to be investigated for total lightning characteristics, nor have they been compared to a large sample of non-tornadic storms. Additionally, while supercell thunderstorms have been analyzed for their mesocyclone-lightning relationships, quasi-linear convective systems (QLCSs), which also produce tornadoes, have not. This study will collect a large sample of tornadic and non-tornadic lightning-producing cells in several tornadic environments across the Southeast U.S. and Oklahoma of mixed storm modes. Flash rates and lightning jumps will be observed to compare and contrast characteristics between tornado production, storm mode, and environments of all cells. Flash rates and jumps will also be scrutinized in tornado-producing cells to analyze any potential temporal relationships between lightning jumps and tornadogenesis.

2. DATA AND METHODS

2.1 Lightning Data

Total lightning data was collected from lightning mapping arrays (LMAs), which are ground-based instruments that locate very high frequency (VHF) radiation from lightning discharges (Rison et al. 1999). Using at least 6 VHF receivers spread out across 50-100 km, they triangulate the location of VHF emissions in four dimensions to map lightning flash channels with typically greater than 95% detection efficiency within 100 km of the network (Rison et al. 1999; Chmielewski and Bruning 2016). We use the lmatools algorithm (deeplycloudy 2015) to take the VHF source data and group individual flashes, their initiation locations, and their initiation times, in addition to flash extent density grids (FED) on a 1 km x1 km x 1 minute grid. FED calculates how many independent lightning flashes pass through each grid space in a time interval. Sources grouped into flashes were required to have a maximum reduced chi-squared value of one, be within a distance threshold of 3 km, a time threshold of 0.15 s, and produce a maximum flash duration of 3 s.

Twelve tornado events were selected for study: eight from the Propagation, Evolution, and Rotation of Linear Storms (PERiLS) deployments in 2022-2023, and four events detected by the OKLMA in 2018-2023 (Koshiba et al. 2024; Table 1). Lightning was only analyzed in areas with high (90-100%) flash detection efficiency (FDE) and almost always in areas of peak (95%-100%) FDE, as determined by Monte Carlo simulations based on the station thresholds for each case (Chmielewski and Bruning 2016). Since FDE maps were not available for any Oklahoma cases, a 100 km range from the OKLMA centroid was always used because that is the region with a high confidence of >95% FDE (Chmielewski and Bruning 2016).

2.2 Cell Tracking, Thresholds, and Size Determination

Cells were identified and mapped using the Python Tobac tracking algorithm (Heikenfeld et al. 2019), which tracks features with gridded data. The variable used to track cells was 5-minute average lightning FED. Lightning variables can then be plotted for individual cells over their life cycle. We note that “cell” here inherently means a lightning-producing cell, and not all storms or storm regions are necessarily captured by this definition. The minimum threshold of flashes per minute over a five minute window for cell detection was altered case-by-case to best capture the cells, meaning that on days with limited flash rates, the threshold was lowered substantially (Table 1). The sigma threshold, which is the standard deviation of a Gaussian distribution used to smooth the FED data for the Tobac algorithm, was also altered to best identify cell tracks (Table 1).

Tobac cell tracks need to be modified to represent the true cell tracks, which includes merging tracks from individual cells that were identified as separate cells, and removing erroneous or short-lived cell tracks (Figure 1). Cells that lasted for less than 15 minutes were removed. The lightning jump algorithm requires at least 12 minutes of flashes to identify a lightning jump, so short-lived cells are of little use (Gatlin 2006; Schultz et al. 2009). Tobac cell tracks were adjusted manually to fit the true cell tracks by analyzing the progression of locally high FED clusters. In addition to using FED grids to adjust cell tracks, the National Weather Service’s dual-polarization, S-band WSR-88D radar data were utilized to confirm and modify cell tracks. WSR 88Ds were also used to assign a storm mode to each cell (supercell, QLCS, etc.).

A radius was subjectively determined that fit the elevated FED cluster associated with each cell, assuring that lightning flashes were properly assigned to their respective cells. Any flash which initiated within this radius was assigned to the respective cell.

Table 1:
The parameters adjusted for each case date. The first 8 cases are PERiLS deployments, while the last 4 are days observed by the OKLMA network in Central Oklahoma. The range from the LMA centroid from which cells were tracked is included, noting that some cases include contributions for the Northern Alabama LMA (NALMA; 03/31/23, 04/05/22). The final two parameters are Tobac parameters adjusted on a case-by-case basis.

Case Date	Range (km)	Threshold (Flashes/Min)	Sigma Threshold (std)
3/22/22	100	4.5	0.0
3/30/22	100	4.5	0.0
04/05/22	175	2.0	1.5
04/13/22	100	1.5	1.0
02/16/23	175	1.5	1.5
03/02/23	175	1.0	1.5
03/24/23	100	4.5	0.0
03/31/23	200	3.5	2.5
05/20/19	100	1.0	5.5
05/25/19	100	2.0	5.5
02/26/23	100	4.5	1.5
05/11/23	100	3.0	1.0

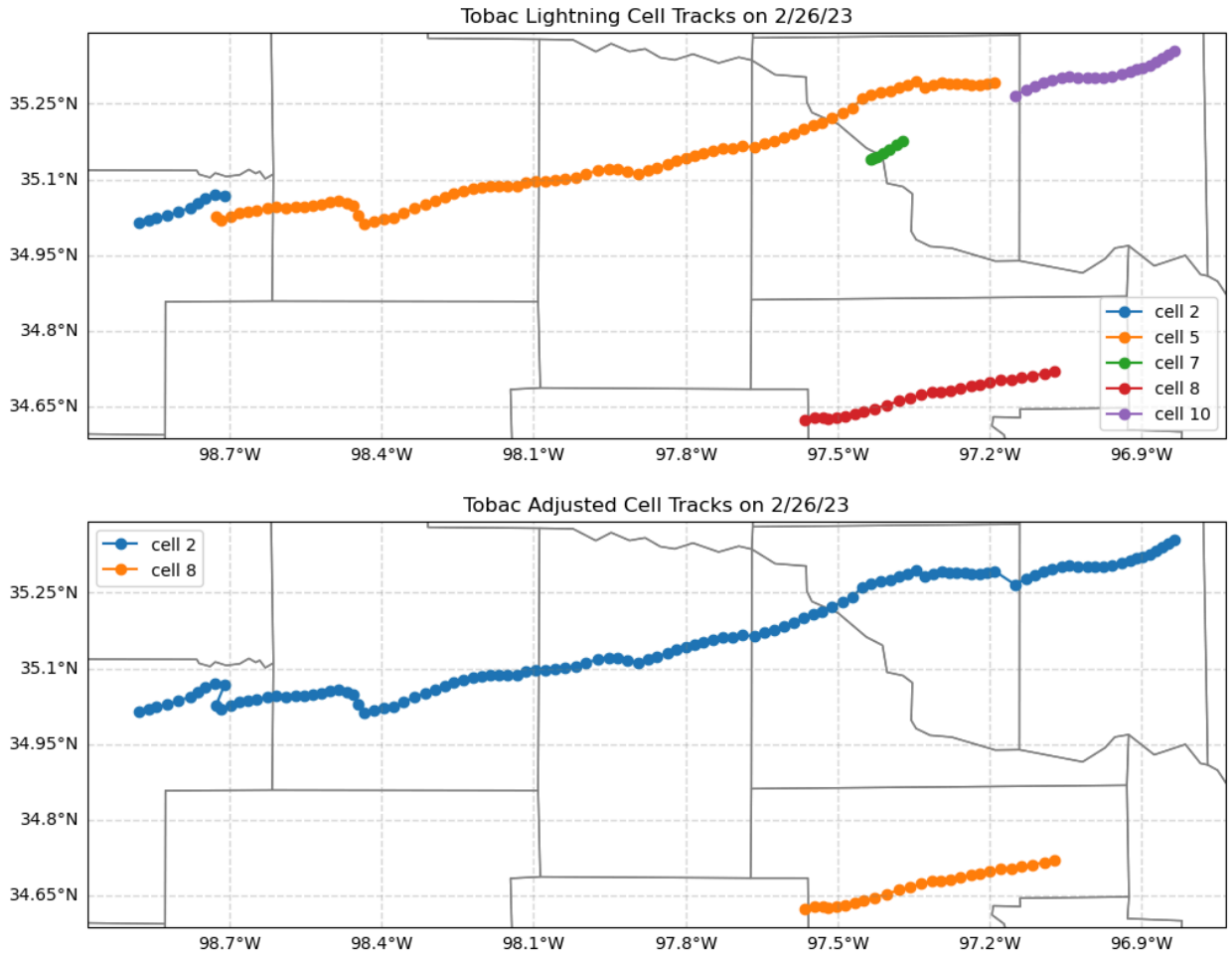

Figure 1: (Top) Raw Tobac tracks from the 2/26/23 case. (Bottom) Manually adjusted tracks. A short track (cell 7) was removed, while three other tracks (cells 2, 5, and 10) were merged into a single track based on FED and radar evolution.

2.3 Lightning Jump Algorithm

A 2σ lightning jump algorithm was used to define lightning jumps, as it was found to be a strong indicator of severe weather compared to other algorithms (Schultz et al. 2009). One minute flash rates are calculated, which are then used to find the change in total flash rate with time (DFRDT) (Gatlin 2006). The standard deviation of DFRDT is found from the previous ten minutes of total lightning. A lightning jump occurs when the DFRDT from the last two minutes is at least two standard deviations above the DFRDT of the prior ten minutes (Schultz et al. 2009). The jump continues until DFRDT is negative, or merged with the following if another jump occurs within six minutes.

2.4 Tornado Data and Cell Attribution

Tornadoes were identified with the Tornado Archive website, which is a reliable database of tornado tracks, including timing and intensity (Maas et al. 2024). All tornado tracks used in this study from the Tornado Archive were sourced from SPC and/or NCEI databases. Tracked cells were assigned tornadoes by collocating the lightning cells with tornado tracks and the corresponding radar reflectivity and velocity fields.

2.5 Identifying Rotation

Low-level rotation was identified with each cell using the azimuthal shear product of the Multi-Radar Multi-Sensor (MRMS) system. Azimuthal shear computes the rotational component of radial velocity radar measurements (Smith et al. 2016). Azimuthal shear was recorded during the entirety of each cell track. Azimuthal shear was attributed to a given cell using the same radius that was defined when grouping flashes to cells for consistency. All azimuthal shear within a respective cell's radius was assigned to it. Each cell's maximum 0-2 km azimuthal shear with time was recorded.

2.6 Defining Non-Tornadic Cells and a Comparable "Tornadogenesis" for Non-Tornadic Cells

To compare tornadic and non-tornadic cells, the non-tornadic cells were required to be substantive and could be seen to pose an eventual tornado risk. Thus, the non-tornadic cells had to meet two conditions to be included in the non-tornadic sample. First, the cell track had to last at least 30 minutes to ensure there was enough time to observe trends in flashes and jumps. Second, the cell had to meet a minimum threshold of maximum azimuthal shear of 0.01 s-1 at some point in its lifecycle (Stough et al. 2017; Pardun 2023). After filtering the non-tornadic cells, the sample was left with 19 storms. Most storms were thought to pose a tornado threat by the NWS in real-time, with 11 cells being associated with at least one Tornado Warning, and another 5 being associated with a Severe Thunderstorm Warning with a "Tornado… Possible" tag.

In the analysis, lightning flash rates and jumps are compared relative to the start time of the tornadoes. Therefore, a similar start time must be assigned to the non-tornadic cells for comparison (e.g., Pardun 2023). Of course, the non-tornadic cells did not produce a tornado, so the azimuthal shear surrounding the tornadoes was used as a reference. In a sample of 31 tornadoes, 0-2 km azimuthal shear on average peaked 7 minutes after tornadogenesis (Figure 2). Therefore, for the non-tornadic cells, "tornadogenesis time" was defined as the time 7 minutes prior to peak 0-2 km azimuthal shear.

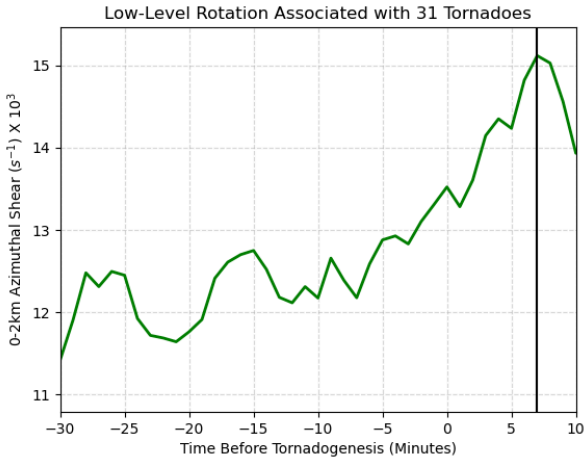

Figure 2: The average rotation of cell tracks associated with 31 tornadoes from all cases after 2019. 0 minutes on the x-axis corresponds to the time of tornadogenesis for all tornadoes. As denoted by the black line, 0-2 km azimuthal shear peaks 7 minutes after the time of tornadogenesis in this sample.

3. RESULTS

The primary objective of this analysis was to compare the total lightning flash rate characteristics of a diverse array of cells in tornadic environments. This was done in three parts. First, a comparison of 2σ lightning jumps with tornadic and non-tornadic cells. Next the total lightning of tornadoes and non-tornadic peaks in low-level rotation were analyzed. Last, the total lightning trends in the minutes before and surrounding tornadogenesis were investigated further.

3.1 Lightning Jumps

A sample of 25 EF1+ tornadoes separated by 30+ minutes in 23 cells was investigated for lightning jumps. If a jump occurred 45 minutes or less before a tornado, it was defined as preceding a tornado (Figure 3). If a jump occurred 45 minutes before the "equivalent tornadogenesis" time, which is 7 minutes before peak 0-2 km azimuthal shear, it was defined as preceding the peak in low-level rotation (Figure 4). For tornadoes preceded by multiple lightning jumps, the closest jump to tornadogenesis was used. Only 15% of lightning jumps were not during or followed by a tornado. Similarly, only 20% of tornadoes were not preceded by a lightning jump (Figure 3). For the

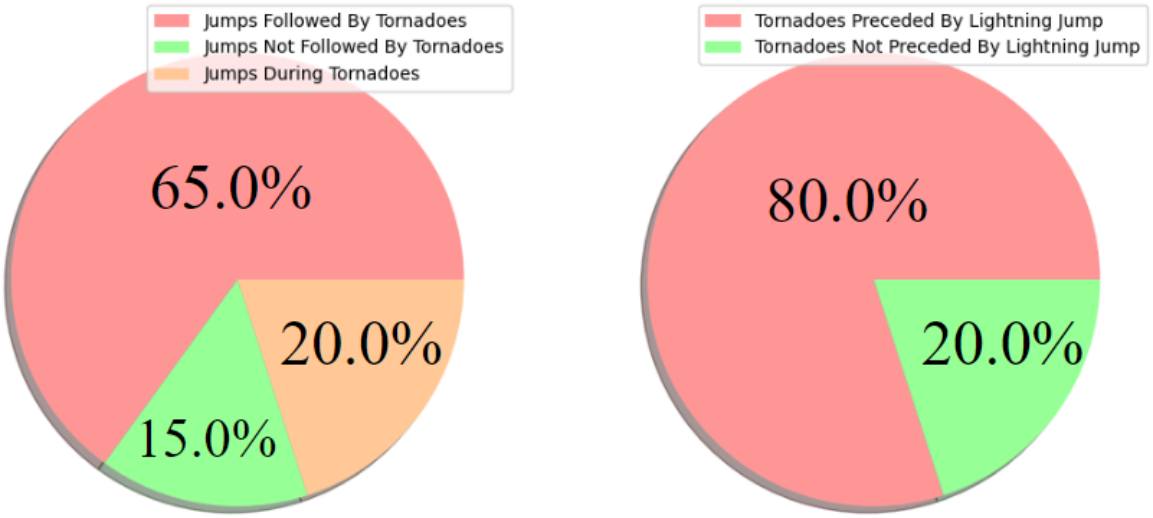

Figure 3: Breaking down the temporal relationship between lightning jumps and tornadoes with a jump-relative perspective (left) and a tornado-relative perspective (right).

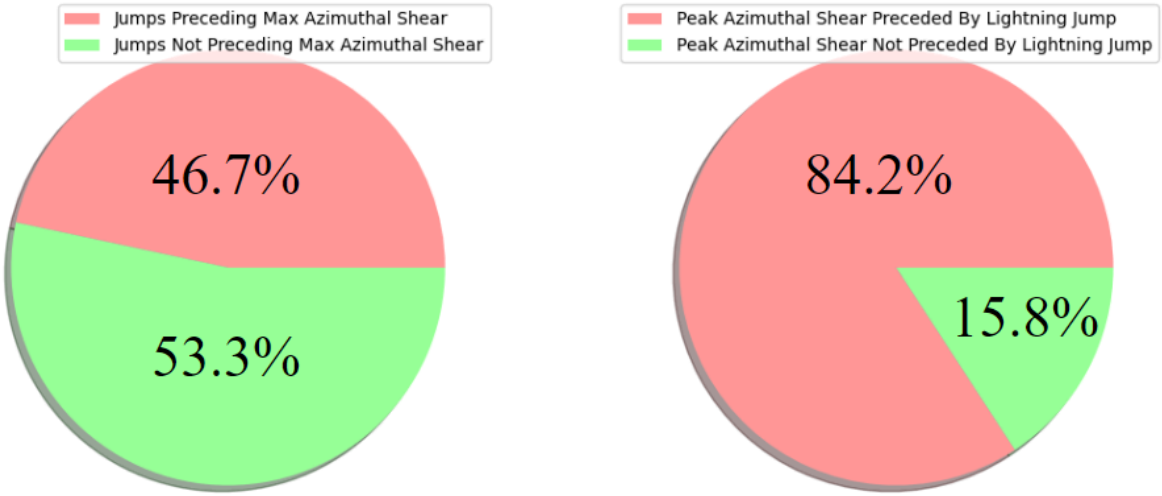

Figure 4: Same breakdown as Figure 3, but instead comparing the temporal relationship of lightning jumps and peaks in 0-2 km azimuthal shear in 19 non-tornadic cells.

20 tornadoes analyzed that were preceded by a lightning jump, a majority of lightning jumps occurred 15-35 minutes before the tornado (Figure 5).

A key interest was seeing if the behavior of lightning jumps in tornadic cells varied from their non-tornadic counterparts. A similar percentage of non-tornadic peaks in rotation were preceded by lightning jumps as their tornadic counterparts (Figure 4). However, in non-tornadic cells, a majority of lightning jumps did not precede the peak in low-level rotation (Figure 4). When

comparing the lightning jumps between the sample of 23 tornadic cells and 19 non-tornadic cells, the tornadic cells averaged 1.74 jumps, while the non-tornadic cells actually had a higher average of 2.37 jumps. Using lightning jumps as a predictor of tornadoes would have a high false alarm rate, but investigating lightning jumps was only the first step of studying the flash rates with these storms.

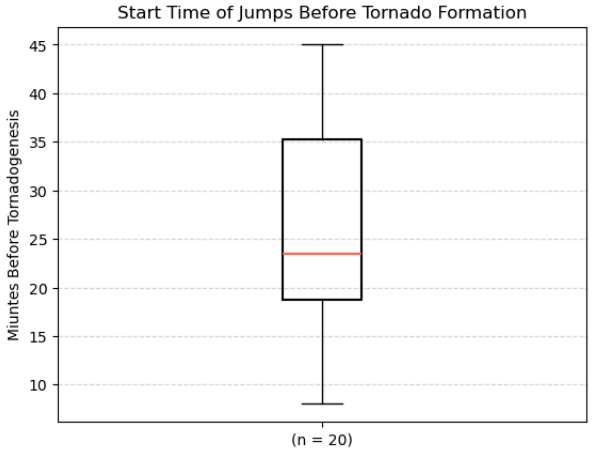

Figure 5: The time of the start of the lightning jump before tornadogenesis. The median pre-tornado jump start time is 23.5 minutes, with an interquartile range of 16.5 minutes.

3.2 Comparing Tornadoes and Non-Tornadic Rotation

A sample of 31 tornadic time periods was compared to the peak of low-level rotation in 19 non-tornadic cells. Both samples have data tracking through the 25-0 minute period before tornadogenesis/equivalent tornadogenesis, so that was the time interval analyzed. The 31 tornadoes are of all intensities separated by at least 15 minutes if they occurred within a single cell. Although including EF0 and cyclic tornadoes was initially a concern, it was justified by noting that the trends in lightning flash rates between the more and less conservative samples were statistically similar (Figure 6).

The differences between the two samples was notable. First, the flash rates preceding tornadogenesis were higher than their non-tornadic counterparts (Figure 7) by a statistically significant margin. The average flash rate of each cell in the 25-0 minute time frame was taken from both samples (Figure 8) and a t-test was conducted on the samples of average flash rates. With a p-value of 0.026 (<0.05), the difference in average total flash rates before the time of (equivalent) tornadogenesis is statistically significant. The low-level rotation before the tornadoes was also higher (Figure 9). The same procedure was conducted on the rotation of the two samples, and with a p-value of 0.0052, the low-level rotation was also significantly higher before tornadogenesis than the non-tornadic maximum in low-level rotation.

The flash rates of each cell in the two samples were normalized to better visualize the relative changes in flash rates, given that flash rates between the cells vary. For each minute in each cell, the flash rate was divided by the maximum flash rate reached by the cell. The maximum normalized flash rate for each cell is one. The normalized flash rates prior to tornadogenesis increases steadily between 25 and 17 minutes, while the increase in the non-tornadic cells is not as substantial (Figure 10). Taking a closer look at flash rates surrounding tornadogenesis would further support the observed trends in flash rates.

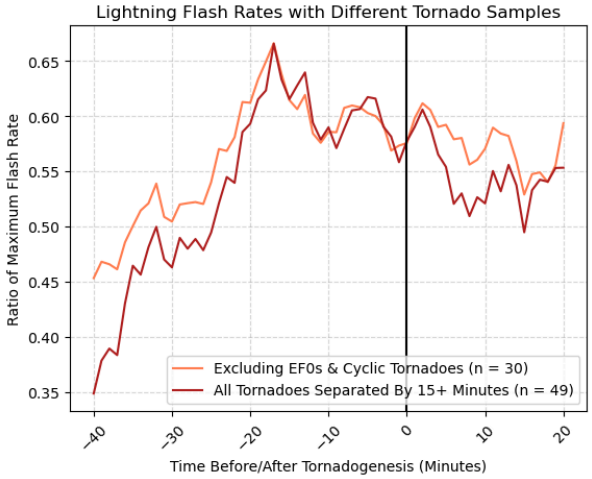

Figure 6: The normalized lightning flash rates of a larger sample of tornadoes also including EF0 and cyclic tornadoes are similar to a sample excluding them, especially in the 25-0 minute timeframe scrutinized in the analysis comparing tornadic and non-tornadic storms.

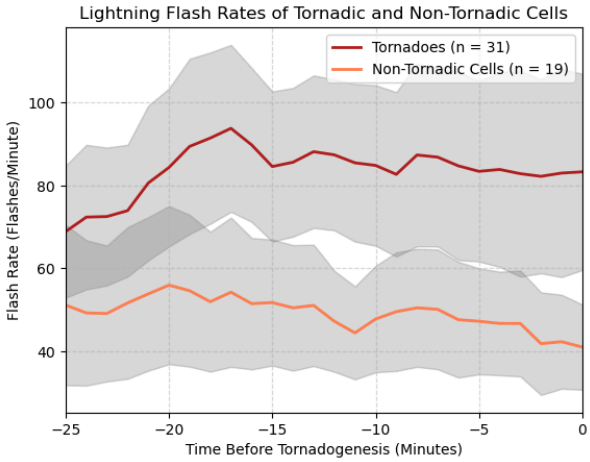

Figure 7: Comparison of flash rates for tornadic and non-tornadic samples in the 25 minutes preceding tornadogenesis (or equivalent tornadogenesis). Shaded is the 95% confidence intervals for each dataset.

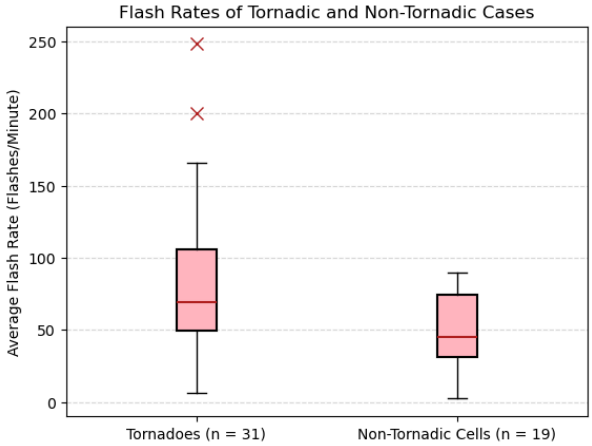

Figure 8: Box plots of the average flash rates in the same 25-minute windows of each cell. Outliers are denoted by the x's and are defined as being more than 1.5 IQRs greater than the third quartile or less than 1.5 IQRs below the first quartile.

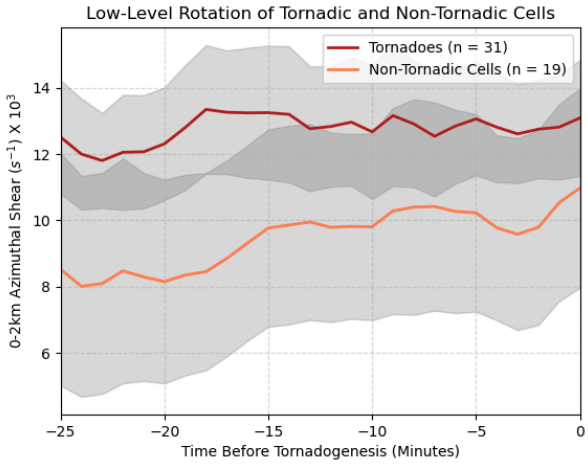

Figure 9: Same as Figure 7, but comparing low-level rotation.

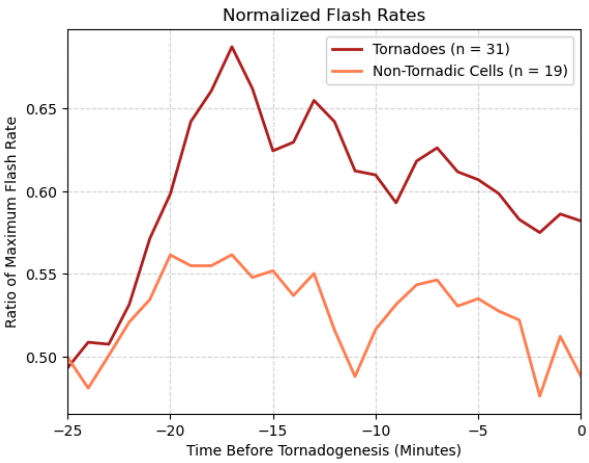

Figure 10: The average normalized flash rates of all tornadoes/non-tornadic cell rotation.

3.3 Investigating Flash Rates Before and Surrounding Tornadogenesis

A larger sample of tornadoes was utilized for this portion of the analysis because tornadoes were used from two Oklahoma cases in 2019 that azimuthal shear was not retrieved for, and thus could not be used for the prior analysis. A similar trend is noticed as in Figure 10: normalized flash rates increase steadily (regardless of whether or not a lightning jump were identified), peak around 17 minutes before tornadogenesis, and then plateau or even decrease slightly (Figure 11). The flash rates were further analyzed for statistical significance.

Two time periods were compared for their flash rates: 30-17 minutes before tornadogenesis,

and 17 minutes before-10 minutes after tornadogenesis. The 17-minute mark was the divider because that was the peak in flash rates across the sample (Figure 11). For each tornado with flash rates collected throughout the entire period, a linear regression was run on the flash rates to find the slope in each time period. The slope in the first time period was positive, while it was near zero in the second time period (Figure 12). The difference in the slopes across the two time period samples was statistically significant, with a p-value of 1.2310-5.

When comparing storm modes, the trends in flash rates surrounding tornadoes in supercells, embedded supercells, and QLCS-embedded cells were similar (Figure 13). Embedded supercells were grouped with QLCS cells, but the two samples were still similar when embedded supercells were grouped with supercells (not shown). When comparing weak and strong tornadoes, there were differences in the flash rate trends (Figure 14). The time before and surrounding weak tornadoes displayed similar trends in flash rates observed in the entire sample (Figure 11), likely because they made up a majority of the sample. Total lightning before strong tornadoes did not increase until closer to tornadogenesis, and remained near maximum levels through tornadogenesis (Figure 14). However, no differences were found to be statistically significant.

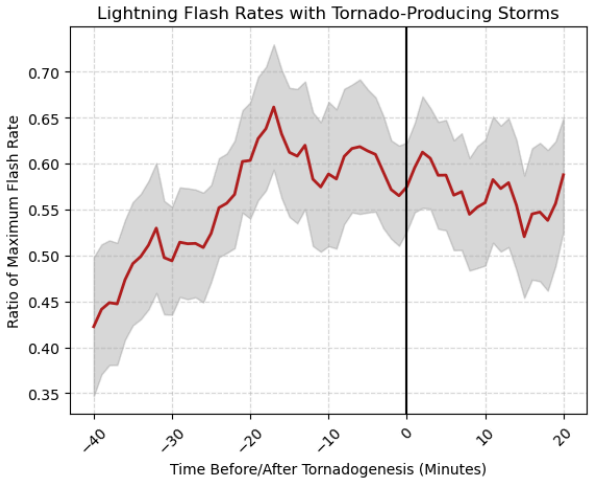

Figure 11: Average normalized flash rates associated with 48 tornadoes. Shaded is the 95% confidence interval. Not all tornadoes have data ranging the entire -40-20 minute span, especially in the minutes farther away from tornadogenesis.

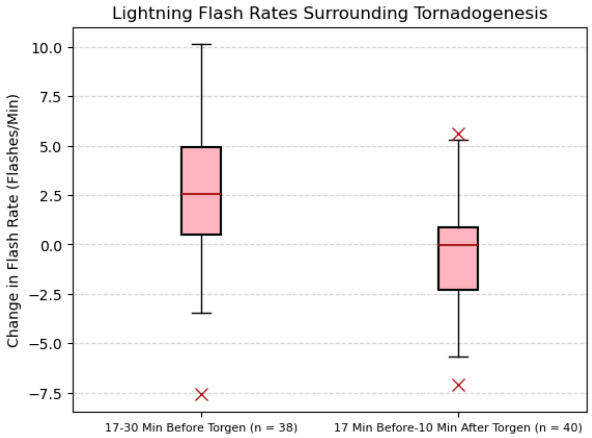

Figure 12: The change in flash rates preceding and surrounding tornadogenesis. Outliers have the same definition as in Figure 6. The median change in flash rates in the 17-30 minute window is 2.6 flashes/minute, with a Q1-Q3 of 0.5-4.9 flashes/minute. The median change in flash rates in the 17 minutes before-10 minutes after tornadogenesis window is 0.0, with a Q1-Q3 of -2.3-0.9.

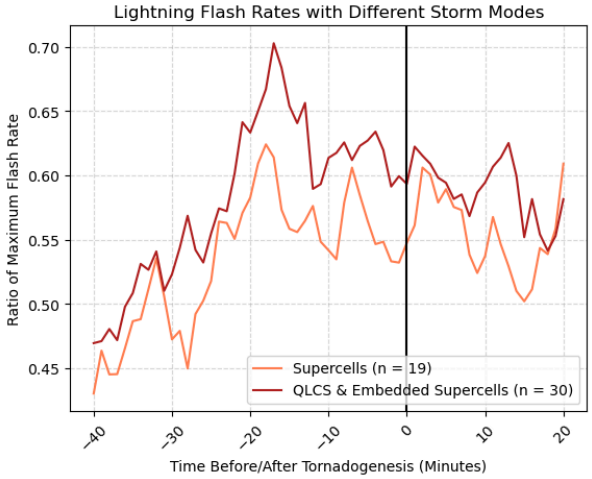

Figure 13: Normalized flash rates of tornadoes with varying storm modes. Flash rates of both samples increase, peak 15-20 minutes before tornadogenesis, and level-off.

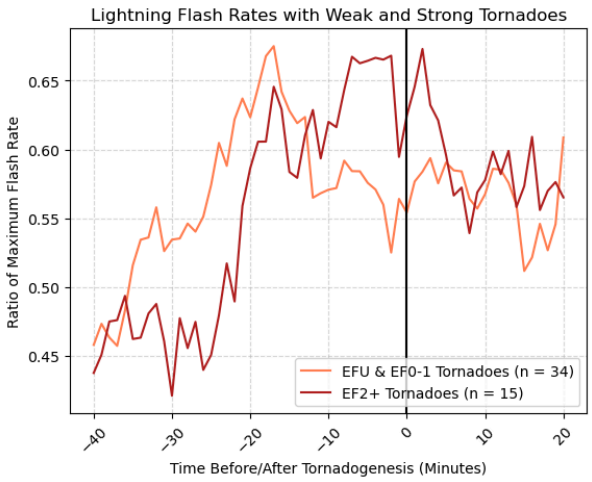

Figure 14: Normalized flash rates of weak/unrated and strong tornadoes. The weak tornadoes display the same trend in flash rates noted previously, while the increase and peak in flash rates with strong tornadoes occur at different times.

4. DISCUSSION

If using the 2σ lightning jump as a predictor of tornadoes in this sample of storms, it would have a false alarm rate of over 74.4%, given that non-tornadic storms had more lightning jumps than their tornadic counterparts. While this rate is quite comparable to reported tornado warning FARs in past years of roughly 75%, it should be noted that these cases were strongly biased towards tornado-producing environments, so if lightning jumps were employed on all severe weather days, the FAR for tornado production would likely be much higher (Lim et al. 2019). More importantly, lightning jumps occurred in the sample of non-tornadic storms at a higher rate than in tornadic storms. These results verify the hypothesis that lightning jump occurrence would not discriminate between tornadic and non-tornadic cells. The 2σ lightning jump algorithm only takes into account the change in flash rates compared to the flash rate variability in 2 min intervals, which is only part of the equation. The magnitude of total lightning, and the duration of a rapid increase in flash rates, are also important indicators of updraft strength (Schultz et al. 2015). Figure 15 shows flash rates with a cell and two lightning jumps. Clearly, the second lightning jump is small in magnitude and slightly shorter in duration. Operationally, this would be a negligible increase in flash rates and likely not considered a lightning jump of interest, but it is a 2σ lightning jump from the preceding variability. The inability for a 2σ lightning jump to capture the intensity and duration of flash rate increases, plus the overall magnitude of total lightning with a storm, was why flash rates irrespective of jumps were analyzed more thoroughly.

A crucial component in supercell tornadogenesis is the strength of the mesocyclone, which is closely related to the midlevel updraft. Mesocyclones develop from updrafts tilting horizontal vorticity from environmental vertical wind shear into the vertical. The mesocyclone is strongest in the midlevel updraft. Mesocyclone strength is modulated by what degree environmental vorticity is tilted and stretched, which is dependent on vertical velocities in the updraft, and those updrafts tend to be strongest at midaltitudes (Markowski and Richardson 2014). Vertical vorticity forming the tornado cyclone is thought to arise from near-surface processes independent of the rotation of the midlevel mesocyclone (Markowski and Richardson 2014). However, to intensify that vertical vorticity by several orders of magnitude to form a tornado, it must be stretched under the mesocyclone. Vorticity is lifted and stretched via the vertical perturbation pressure gradient, the acceleration of which points upward towards the low pressure of the mesocyclone (Markowski and Richardson 2014). With the tornado partially dependent on mesocyclone strength, which is dependent on midlevel updraft strength, a connection can be drawn to total lightning.

A storm's propensity to produce a tornado is indirectly related to midlevel updraft strength through the midlevel mesocyclone. Similarly, total flash rate and lightning jumps are correlated with variables denoting updraft strength (Schultz et al. 2015). If lightning flash rates and tornadogenesis are both modulated by midlevel updraft intensity, then that could serve as a possible explanation for some of the results. Tornadoes averaged higher flash rates before tornadogenesis than non-tornadic cells, a potential sign of a stronger mesocyclone. The prolific increase in total lightning in the 15-30 minutes preceding tornadogenesis could be a sign that the midlevel mesocyclone is rapidly organizing in association with the updraft. However, a significant number of tornadoes in the sample were produced by QLCSs, whose processes for tornadogenesis are different and less understood than supercells. Yet,

trends in total lightning were similar surrounding tornadoes regardless of storm mode.

Two primary QLCS tornadogenesis processes are with a mesocyclone, similar to supercells, and via the release of horizontal shearing instability (HSI) (Goodnight et al. 2022). Marion and Trapp (2021) found that QLCS tornado strength is correlated to low-level updraft width, but less so the strength of the updraft. Moreover, the depth of the updraft was not significant. This study did not address the temporal relationship of updraft strength and tornadogenesis. The results in our study find a similar increase in lightning flash rates before QLCS tornadogenesis to what is noted in supercells. This might indicate the significance of a strengthening and/or enlarging midlevel updraft that precedes QLCS tornadogenesis in association with the updraft. Perhaps a strengthening midlevel updraft can be associated with a cold pool surge that induces a release of HSI and tornadogenesis (Goodnight et al. 2022).

An area of future research could be to compare lightning flash rates with these cells to different radar characteristics. For example, Kuster et al. (2024) found specific differential phase (K_{DP}) to be a useful tool to help predict QLCS mesovortex formation. Decreases in K_{DP} preceded 95% of mesovortices, while midlevel K_{DP} cores preceded most mesovortices as well. These K_{DP} signatures may be related to surges in the QLCS that are crucial to mesovortex development (Kuster et al. 2024). Both K_{DP} and lightning are influenced by microphysical processes, and since K_{DP} signatures have been shown to be useful in mesovortex prediction, it may be an interesting variable to compare with lightning flash rates.

While this study had a large sample of tornadoes and non-tornadic rotating storms compared to past research, a limitation is still the smaller sample sizes analyzed, particularly of non-tornadic peaks in low-level rotation. There were 19 for each maximum in low-level rotation of 19 non-tornadic cells. Future research could collect larger samples, particularly of non-tornadic storms in similar environments which might be expected to produce tornadoes, to see if the results affirm those in this study. An addition to this study to increase sample size could be to look at multiple maxima in non-tornadic low-level rotation throughout each storm's lifespan. This would mirror the approach taken to tornado observations in this study, where multiple tornadoes from the same cells were analyzed. Future research could also collect and observe data from more days that were not verified as tornado outbreaks to get a larger proportion of non-tornadic cells. Although eight PERiLS deployments and 4 Oklahoma cases were investigated, two of the Oklahoma cases from 2019 did not have MRMS data, and thus weren't looked at when comparing tornadic and non-tornadic flash rates. Furthermore, the two Oklahoma cases used in all analyses only had one non-tornadic cell used in the sample. A key area of future research to expand on this study is to gather a larger and more diverse sample of storms and cases.

There are a couple more limitations to the methods of this study. First, while the method of matching up "tornadogenesis time" with non-tornadic cells was the most appropriate avenue possible, there's no way to accurately match up tornadogenesis times with storms that don't produce tornadoes. Determining the radius of each cell within which to include lightning flashes was manually done and thus at least partially subjective. The sampled storm cells were also defined by the lightning produced, implying that all storm cells had updrafts reaching mixed-phase supportive temperatures. This is a unique aspect of this study, which allows for isolating regions of suspected stronger updraft within the larger QLCS, but lightning itself is not a requirement for a tornado to be produced.

Another area of future research could be to observe other lightning characteristics, like lightning flash area and initiation altitude.

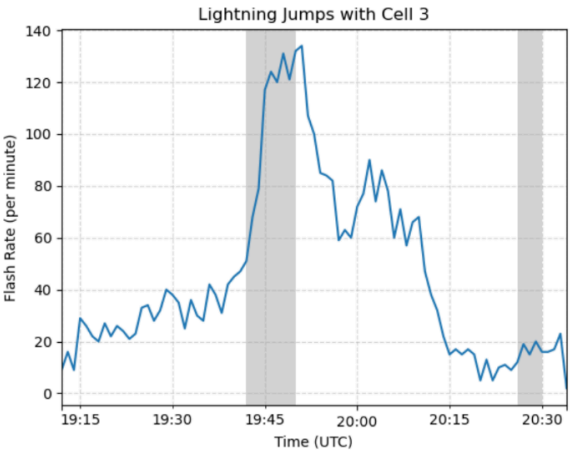

Figure 15: Lightning flash rates and jumps (shaded) with a cell from 3/22/22. The first jump has a peak flash rate more than six times greater than the second.

5. SUMMARY AND CONCLUSIONS

This study was conducted to help fill in the gap of research analyzing lightning flash rates and jumps with tornadoes. It also aimed to compare flash rates between tornado-producing storms and non-tornadic rotating storms, another area of limited research. The study also sought to compare the total lightning before tornadogenesis in supercells and quasi-linear convective systems. Lightning mapping array data was pulled from PERiLS deployments and Oklahoma LMAs for a total of 12 cases. Cells were tracked within range of the LMAs based on flash extent density, which helps isolate regions of interest within a larger QLCS. Nineteen rotating non-tornadic cells were identified and 49 tornadoes were associated with tracked cells. The primary findings were:

- Lightning jumps occurred frequently in tornadic and non-tornadic cells.
- The average total lightning in the 25 minutes before tornadogenesis was significantly higher than the average total lightning preceding peaks in non-tornadic low-level rotation.
- In the time before tornadogenesis, lightning flash rates increased steadily until about 17 minutes before tornado touchdown. At this point they peaked and then plateaued all the way through tornadogenesis.
- Lightning flash rates associated with isolated tornadic supercells and QLCS-embedded cells displayed similar behavior.

A proposed explanation for the higher flash rates in tornadic cells was the importance of a strong midlevel updraft for lightning production and, indirectly, tornadoes. A stronger midlevel updraft could correspond with a stronger midlevel mesocyclone. Likewise, the increase in flash rates preceding tornadogenesis might be attributed to a strengthening updraft and mesocyclone.

Future research should expand on the sample size used in this study to observe if similar findings are detected. If these results are affirmed in future research, study can go into exploring possible explanations for the observations such as the ones proposed in this study. Future research could also compare the observed trends in flash rate to various radar products and signatures that may also be related to tornado formation.

6. ACKNOWLEDGMENTS

Dr. Daphne LaDue and Alex Marmo coordinated the National Weather Center Research Experience for Undergraduates, and without their hard work this research would not be possible. LMA data are available at Chmielewski et al. 2022, 2023, 2023 (b).

This work was prepared by the authors with funding provided by National Science Foundation Grant No. AGS-2050267, and NOAA/Office of Oceanic and Atmospheric Research under NOAA-University of Oklahoma Cooperative Agreement #NA11OAR4320072, U.S. Department of Commerce. The statements, findings, conclusions, and recommendations are those of the author(s) and do not necessarily reflect the views of the National Science Foundation, NOAA, or the U.S. Department of Commerce.

7. REFERENCES

Bruning, E. C., and D. R. MacGorman, 2013: Theory and Observations of Controls on Lightning Flash Size Spectra. J. Atmos. Sci., 70, 4012–4029, https://doi.org/10.1175/JAS-D-12-0289.1.

Calhoun, K. M., D. R. MacGorman, C. L. Ziegler, and M. I. Biggerstaff, 2013: Evolution of Lightning Activity and Storm Charge Relative to Dual-Doppler Analysis of a High-Precipitation Supercell Storm. Mon. Wea. Rev., 141, 2199–2223, https://doi.org/10.1175/MWR-D-12-00258.1.

Chmielewski, V. C., and E. C. Bruning, 2016: Lightning Mapping Array Flash Detection Performance with Variable Receiver Thresholds. J. Geophys. Res. Atmos., 121, 8600–8614, https://doi.org/10.1002/2016JD025159.

Chmielewski, V. C., M. Stock, D. R. MacGorman and D. Kennedy, 2023: Oklahoma Lightning Mapping Array (OKLMA) Level 1 Data. Dataset available online from the NOAA/OAR National Severe Storms Laboratory, Norman, Oklahoma, U.S.A.,

accessed <insert date>, doi:10.15763/DBS.OKLMA.

Chmielewski, V., et al. 2023. PERiLS_2023: NSSL Deployable Lightning Mapping Array Data. Version 1.0. UCAR/NCAR - Earth Observing Laboratory. https://doi.org/10.26023/YNDP-KDMP-5K0G.

Chmielewski, V., et al. 2022. PERiLS_2022: NSSL Deployable Lightning Mapping Array Data. Version 1.1. UCAR/NCAR - Earth Observing Laboratory. https://doi.org/10.26023/R0K6-AXR5-YZ00. Accessed 29 Jul 2024.

deeplycloudy, 2015: lmatools: lmatools-v0.5z-stable. Zenodo, https://doi.org/10.5281/zenodo.32510.

Gatlin, P., 2006: Severe Weather Precursors in the Lightning Activity of Tennessee Valley Thunderstorms. M.S. Thesis, The University of Alabama in Huntsville, 87 pp. [Available online at: https://ams.confex.com/ams/88Annual/techprogram/paper_130298.htm.]

Goodnight, J. S., D. A. Chehak, and R. J. Trapp, 2022: Quantification of QLCS Tornadogenesis, Associated Characteristics, and Environments across a Large Sample. Wea. Forecasting, 37, 2087–2105, https://doi.org/10.1175/WAF-D-22-0016.1.

Heikenfeld, M., P. J. Marinescu, M. Christensen, D. Watson-Parris, F. Senf, S. C. van den Heever, and P. Stier, 2019: tobac 1.2: Towards a Flexible Framework for Tracking and Analysis of Clouds in Diverse Datasets. Geosci. Model Dev., 12, 4551–4570, https://doi.org/10.5194/gmd-12-4551-2019.

Kosiba, K. A., and Coauthors, 2024: The Propagation, Evolution, and Rotation in Linear Storms (PERiLS) Project. Bull. Amer. Meteor. Soc., https://doi.org/10.1175/BAMS-D-22-0064.1, in press.

Kuster, C. M., K. D. Sherburn, V. N. Mahale, T. J. Schuur, O. F. McCauley, and J. S. Schaumann, 2024: Radar Signatures Associated with Quasi-Linear Convective System Mesovortices. Wea. Forecasting, https://doi.org/10.1175/WAF-D-23-0144.1, in press.

Lim, J. R., B. F. Liu, and M. Egnoto, 2019: Cry Wolf Effect? Evaluating the Impact of False Alarms on Public Responses to Tornado Alerts in the Southeastern United States. Wea. Climate Soc., 11, 549–563, https://doi.org/10.1175/WCAS-D-18-0080.1.

Maas, M., T. Supinie, A. Berrington, S. Emmerson, A. Aidala, and M. Gavan, 2024: The Tornado Archive: Compiling and Visualizing a Worldwide, Digitized Tornado Database. Bull. Amer. Meteor. Soc., 105, E1137–E1152, https://doi.org/10.1175/BAMS-D-23-0123.1.

Marion, G. R., and R. J. Trapp, 2021: Controls of Quasi-Linear Convective System Tornado Intensity. J. Atmos. Sci., 78, 1189–1205, https://doi.org/10.1175/JAS-D-20-0164.1.

Markowski, P. M., and Richardson Y. P., 2014: The Influence of Environmental Low-Level Shear and Cold Pools on Tornadogenesis: Insights from Idealized Simulations. J. Atmos. Sci., 71, 243–275, https://doi.org/10.1175/JAS-D-13-0159.1.

Markowski, P. M., and Richardson Y. P. , 2009: Tornadogenesis: Our Current Understanding, Forecasting Considerations, and Questions to Guide Future Research. Atmos. Res., 93 , 3–10, https://doi.org/10.1016/j.atmosres.2008.09.015.

Pardun, T., 2023: An Investigation Between Tornadic and Non-Tornadic QLCS Mesovortices using Operational and Experimental MRMS Products. M.S. Thesis, School of Meteorology, The University of Oklahoma, 109 pp. [Available online at: https://shareok.org/handle/11244/338758.]

Perez, A. H., L. J. Wicker, and R. E. Orville, 1997: Characteristics of Cloud-to-Ground Lightning Associated with Violent Tornadoes. Wea. Forecasting, 12, 428–437, https://doi.org/10.1175/1520-0434(1997)012<0428:COCTGL>2.0.CO;2.

Rison, W. , Thomas R. J., Krehbiel P. R., Hamlin T., and Harlin J. (1999), A GPS-Based Three-Dimensional Lightning Mapping System: Initial Observations in Central New Mexico, Geophys. Res. Lett., 26, 3573–3576, doi:10.1029/1999GL010856.

Schultz, C. J., L. D. Carey, E. V. Schultz, and R. J. Blakeslee, 2015: Insight into the Kinematic and Microphysical Processes that Control Lightning Jumps. Wea. Forecasting, 30, 1591–1621, https://doi.org/10.1175/WAF-D-14-00147.1.

Schultz, C. J., W. A. Petersen, and L. D. Carey, 2011: Lightning and Severe Weather: A Comparison between Total and Cloud-to-Ground Lightning Trends. Wea. Forecasting, 26, 744–755, https://doi.org/10.1175/WAF-D-10-05026.1.

Schultz, C. J., W. A. Petersen, and L. D. Carey, 2009: Preliminary Development and Evaluation of Lightning Jump Algorithms for the Real-Time Detection of Severe Weather. J. Appl. Meteor. Climatol., 48, 2543–2563, https://doi.org/10.1175/2009JAMC2237.1.

Smith, T. M., and Coauthors, 2016: Multi-Radar Multi-Sensor (MRMS) Severe Weather and Aviation Products: Initial Operating Capabilities. Bull. Amer. Meteor. Soc., 97, 1617–1630, https://doi.org/10.1175/BAMS-D-14-00173.1.

Stough, S. M., L. D. Carey, C. J. Schultz, and P. M. Bitzer, 2017: Investigating the Relationship between Lightning and Mesocyclonic Rotation in Supercell Thunderstorms. Wea. Forecasting, 32, 2237–2259, https://doi.org/10.1175/WAF-D-17-0025.1.

Takahashi, T., 1978: Riming Electrification as a Charge Generation Mechanism in Thunderstorms. J. Atmos. Sci., 35, 1536–1548, https://doi.org/10.1175/1520-0469(1978)035<1536:REAACG>2.0.CO;2.

Williams, B. M., and L. D. Carey, 2015: Assessing the Utility of Total Lightning and the Lightning Jump to Assist in the QLCS Tornado Warning Decision Process. Preprints, *95th American Meteorological Society Annual Meeting*, Phoenix, AZ, Amer. Meteor. Soc., 11.3. [Available online at: https://ams.confex.com/ams/95Annual/webprogram/Paper259488.html.].

Williams, E. R., and Coauthors, 1999: The Behavior of Total Lightning Activity in Severe Florida Thunderstorms, Atmos. Res., 51, 245-265, https://doi.org/10.1016/S0169-8095(99)00011-3.